Nano-Storage Wires

Dong Jun Lee,[†] Eunji Kim,[†] Daesan Kim,[†] Juhun Park,[‡] and Seunghun Hong[†,‡,*]

[†]Department of Biophysics and Chemical Biology, Seoul National University, Seoul, 151-747, Korea and [‡]Department of Physics and Astronomy, Seoul National University, Seoul 151-747, Korea

ABSTRACT We report the development of "nano-storage wires" (NSWs), which can store chemical species and release them at a desired moment *via* external electrical stimuli. Here, using the electrodeposition process through an anodized aluminum oxide template, we fabricated multisegmented nanowires composed of a polypyrrole segment containing adenosine triphosphate (ATP) molecules, a ferromagnetic nickel segment, and a conductive gold segment. Upon the application of a negative bias voltage, the NSWs released ATP molecules for the control of motor protein activities. Furthermore, NSWs can be printed onto various substrates including flexible or three-dimensional structured substrates by direct writing or magnetic manipulation strategies to build versatile chemical storage devices. Since our strategy provides a means to store and release chemical species in a controlled manner, it should open up various applications such as drug delivery systems and biochips for the controlled release of chemicals.

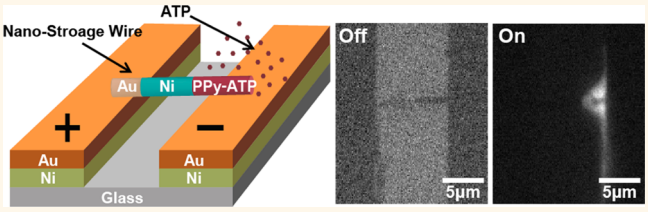

KEYWORDS: nanowire · polypyrrole · controlled release · printable · bioenergy storage · nano−bio interface

The activity of *protein* molecules is inherently controlled by *chemical* molecules that act as activation signals or energy sources.[1] For example, biomotors require adenosine triphosphate (ATP) to generate force and motion in living cells.[2] Various applications such as biochips[3,4] and biosensors[5,6] have been relying on such interactions between proteins and chemical molecules. Thus, it is of great importance to develop technologies for the controlled release of signaling chemical molecules in the fabrication of devices relying on protein functionalities.[7−16] For example, the "caged ATP" method utilized UV-active compounds that can hold ATP and release it in the solution upon exposure to UV light.[14−17] Also, various other methods such as conducting polymer-based devices[8−10] and microfluidic devices[11−13] have been intensively studied for the controlled release of biochemical molecules.[7] However, these methods often suffered from various limitations. For example, previous methods can be utilized to control the biomolecular concentration over the entire solution, but it is often very difficult to control the local concentrations of desired biomolecles.[18,19] Also, many previous methods required macroscopic auxiliary devices[11,14−19] such as pumps and UV-light sources, which cannot be integrated into compact devices for nanomechanical systems. On the other hand, nanoparticles (NPs)[20−22] or nanowires (NWs)[23,24] synthesized from the combination of various materials have been applied to drug delivery systems[20−23] or printable electrical devices[25,26] since the NPs and NWs can be guided to the desired locations by external forces.[25−29] However, nanostructures that can store and release specific chemicals upon electrical stimuli have not been developed yet.

Herein, we developed "nano-storage wires" (NSWs) that can store chemical species and release them when stimulated by an external electrical bias. In this work, electrodeposition techniques[27,30] were utilized to fabricate multisegmented NWs composed of a polypyrrole (PPy) segment containing chemical species such as ATP, a ferromagnetic nickel (Ni) segment, and a conductive gold (Au) segment. Due to the Ni segment, we could drive and deposit the NSWs onto specific regions on electrode surfaces *via* an external magnetic field.[27,28] The NSWs on the electrodes formed a good electrical contact with the electrodes *via* the Au segment, and they released chemical species from the PPy segment[27,31−33] by the external electric potential from the electrodes. As a proof of concept, we demonstrated the control of motor protein activities using NSWs containing ATP. We also showed that NSWs can be printed on flexible or even on 3D structured substrates to build chemical storage devices. Since the NSWs can store

* Address correspondence to seunghun@snu.ac.kr.

Received for review April 25, 2013 and accepted July 16, 2013.

Published online July 16, 2013
10.1021/nn402082v

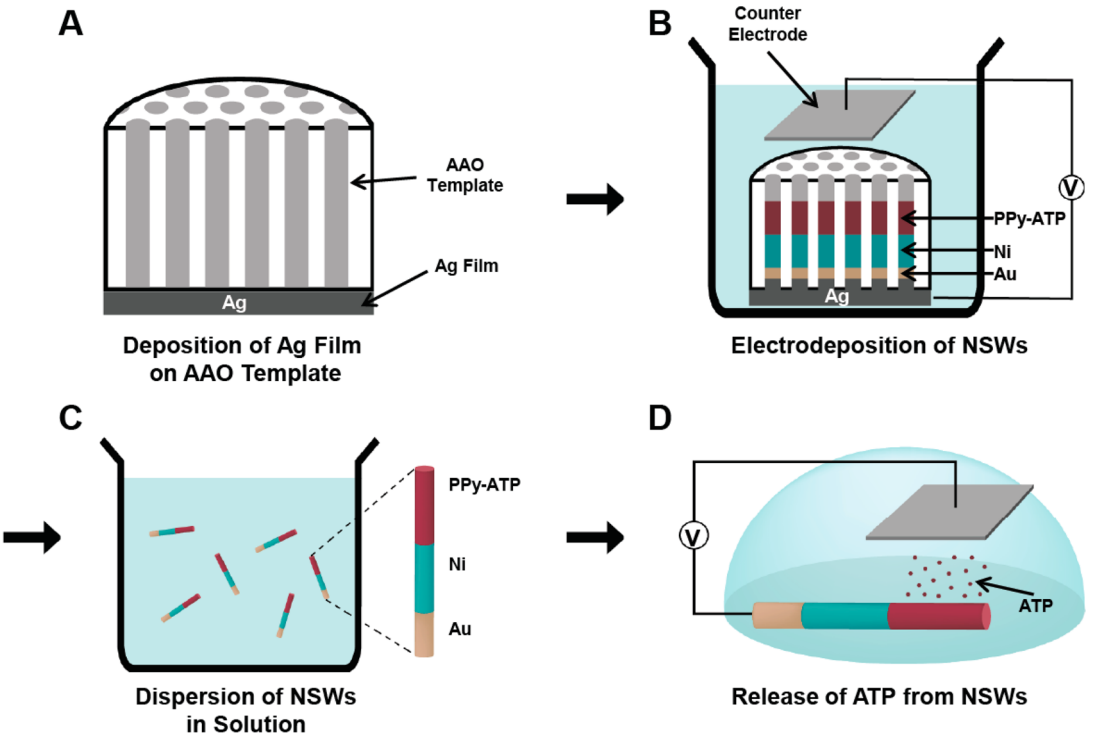

Figure 1. Schematic diagram depicting the fabrication of NSWs. (a) Deposition of Ag onto an AAO template. A 500 nm thick Ag layer was thermally evaporated onto one side of the AAO template to serve as a working electrode. (b) Electrodeposition processes of NSWs. The Au, Ni, and PPy-ATP were electrochemically deposited in series. Yellow, blue, and red segments represent Au, Ni, and PPy-ATP segments, respectively. (c) Dispersion of NSWs into the solution. The Ag layer and the AAO template were removed by nitric acid and 3 M NaOH, respectively. (d) Controlled release of ATP from a NSW by applying a negative bias voltage onto the NSW. A bias voltage of −2 V was applied to the NSWs to release ATP molecules in a controlled manner.

chemical species and release them at any desired moment *via* external stimuli, they can be utilized for various biochip applications such as the controlled delivery of drugs and other chemicals for the control of protein activities.[31]

RESULTS AND DISCUSSION

Figure 1 shows a schematic diagram depicting the fabrication method of nano-storage wires. We fabricated multisegmented NWs composed of Au, Ni, and PPy-ATP segments. The PPy-ATP segment has been utilized for the controlled release of ATP molecules.[8−10] The Ni segment enables the magnetic localization of NSWs,[27,28] while the Au segment provides a good electrical contact with electrodes. When Ni is exposed to air or aqueous conditions, the surface oxidation results in high contact resistance.[34,35] Therefore, the Au segment was incorporated to lower the contact resistance between the NSWs and the electrodes.[36] The detailed procedure for the NSW fabrication method can be found in the Materials and Methods section. In brief, a 500 nm thick silver (Ag) layer was thermally evaporated on one side of an anodized aluminum oxide (AAO) template (Figure 1a) to serve as a working electrode.[30] After the thermal deposition of an Ag layer, additional Ag was electrochemically deposited using a potentiostat to create a uniform working electrode for the deposition of NSWs.[37] The desired Au, Ni, and PPy-ATP segments were deposited in series (Figure 1b). Following the deposition, the Ag backing layer was etched using 70% nitric acid,[38] and then the AAO was dissolved in 3 M NaOH solution[30] to disperse the NSWs in the solution (Figure 1c). Here, only the Ag layer deposited on the side of the AAO template was exposed to the nitric acid, and the Au segment prevents the intrusion of the nitric acid into the Ni and PPy segments. It prevented potential damage to the ATP stored in the PPy parts. Furthermore, since the diffusion of small ions such as NaOH in the solution toward the core of the PPy matrix is negligible,[39,40] most of the ATP molecules can be stored stably within the PPy segment. The dispersed NSWs were thoroughly rinsed with deionized water prior to the release experiments. Figure 1d shows a schematic diagram depicting the measurement of the real-time controlled release of ATP from a NSW. Here, the NSW as well as a counter electrode was placed in the solution of an ATP bioluminescence assay kit containing luciferin and luciferase. When a negative bias voltage of −2 V was applied to the NSW, the PPy-ATP segment in the NSW expanded and released ATP. Due to the released ATP, the luciferin around the NSW was rapidly oxidized by luciferase, producing light. Thus, the observation of such light around the NSW by fluorescence microscopy can be an indication of the ATP release from the NSW.[23]

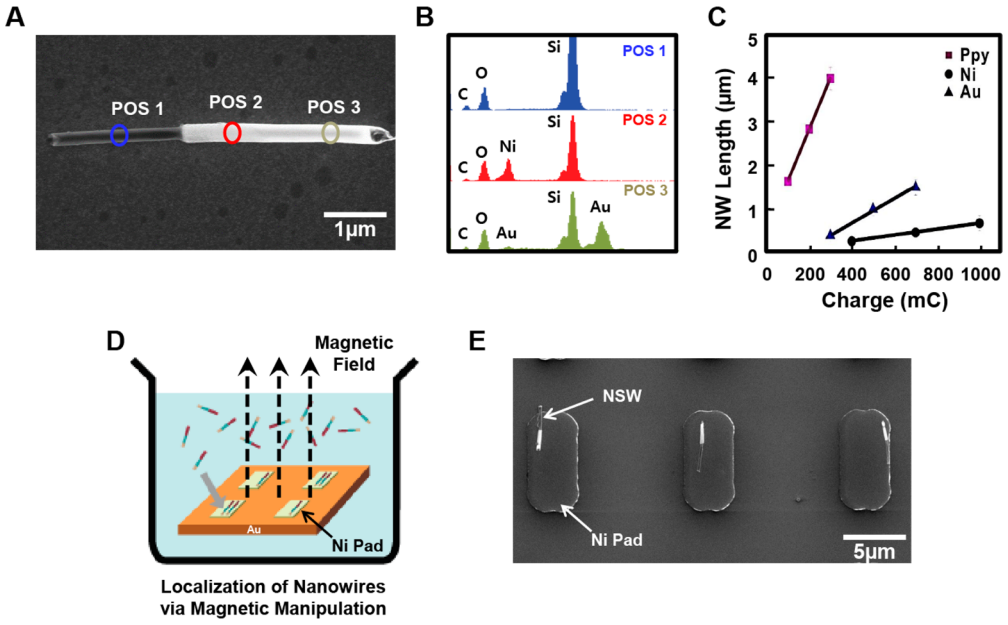

Figure 2. Characterizations of NSWs. (a) SEM image of a single NSW. The dark, intermediate, and bright regions represent PPy-ATP, Ni, and Au segments, respectively. (b) EDS spectra on the NSW. The blue, red, and green spectra correspond to position 1, 2, and 3 of part (a), respectively. (c) Growth length of each segment *versus* applied charges. (d) Schematic diagram depicting the localization of NSWs driven by magnetic fields. NSWs in the solution were attracted to predefined Ni patterns when external magnetic fields were applied. (e) SEM image of NSWs localized on Ni patterns.

Figure 2a shows the scanning electron microscopy (SEM) image of NSWs. The NSW consisted of three distinct segments: dark, intermediate, and bright regions corresponding to PPy-ATP, Ni, and Au segments, respectively. To confirm the chemical compositions of each segment, we performed energy dispersive X-ray spectroscopy (EDS) (Figure 2b). Position 1 (POS1) of the NSW mainly consisted of carbon and oxygen, while positions 2 (POS2) and 3 (POS3) contained Ni and Au, respectively. Strong Si peaks appeared in all regions since the NSWs were loaded onto a silicon oxide wafer for the EDS analysis. These EDS results clearly confirmed that our fabrication method allowed the synthesis of NSWs with discrete segments.

Figure 2c shows the length of each segment with respect to applied charges during electrodeposition. EDS analysis in the line scanning mode was conducted along the long axis of the NSWs to investigate the precise lengths of each segment. The length of each segment linearly correlated with the applied charges. The growth rate was 14 nm/mC for the PPy-ATP segment, 0.9 nm/mC for the Ni segment, and 3.2 nm/mC for the Au segment (Figure 2c). This result implies that we can control the length of each segment simply by controlling the applied charges during the electrodeposition process.

Each segment in a NSW plays a role to extend the applications of the NSWs. The PPy segment stores chemical species such as ATP. The Au segment enables a good electrical contact between the deposited NSWs and the electrodes because Au does not form an insulating oxide layer on it. The Ni segment of the NSWs allows one to utilize magnetic fields to drive the NSWs and place them onto a specific location for device applications. As a proof of concept, we demonstrated the deposition of NSWs onto a specific location on a solid substrate using ferromagnetic Ni patterns (Figure 2d).[27] Here, Ni patterns (5 μm $\times$ 10 μm) on a silicon oxide wafer were placed in the dispersions of NSWs, and an external magnetic field was applied. In this case, the magnetic field around the Ni patterns became larger than other regions, and, thus, the NSWs were driven to the Ni patterns due to its magnetic segment. Figure 2e shows the SEM image of NSWs on ferromagnetic Ni patterns. The NSWs were aligned and localized on the Ni patterns. This result indicated that the position and the alignment of individual NSWs can be controlled by utilizing magnetic fields, which can be utilized to assemble complicated device structures for practical applications.

Figure 3a shows fluorescence micrographs of NSWs with (right panel) and without (left panel) the application of bias voltages as described in Figure 1d. Without a bias voltage, NSWs appeared as dark regions (left panel). When a negative bias voltage was applied, the PPy-ATP segments expanded and released ATP into the solution. The released ATP stimulated the oxidation of luciferin around the NSW, producing light (right panel). Note that although the released ATP could usually diffuse out over a long distance in solution environments,[31] in this experiment, it reacted with nearby luciferase and luciferin immediately and generated fluorescent light only near the NSWs. This result clearly shows that our NSWs could store biochemical

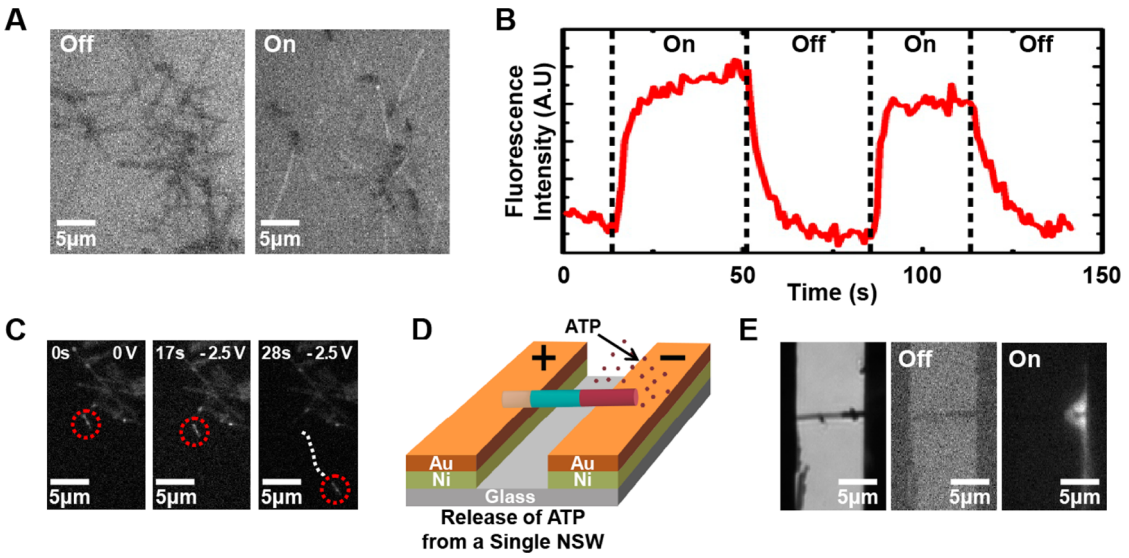

Figure 3. Controlled release of ATP *via* electrical stimuli. (a) Fluorescence images of NSWs on a Au substrate with (right panel) and without (left panel) the application of a −2 V bias voltage. The ATP bioluminescence assay kit (luciferin/luciferase kit from Sigma Aldrich, USA) was used to detect the release of ATP. (b) Graph of the fluorescence intensity with respect to time. The fluorescence intensity indicating ATP molecules was repeatedly increased and decreased with application and removal of −2 V bias voltage, respectively. The data were obtained from the NSWs in (a). (c) Control of biomotor motility using NSWs. Here, the thin Au surface on glass was coated with kinesin biomotors. The white line in the red dotted circle represents a microtubule on the kinesin biomotors. Other white lines represent the NSWs on the substrate. (d) Schematic diagram depicting the controlled release of ATP from an individual NSW between two electrodes. The NSW was magnetically localized onto an electrode consisting of Ni (green) and Au (orange), and then a −2 V bias voltage was applied across the NSWs. (e) Optical (left) and fluorescence image of a single NSW with (right) and without (middle) a −2 V bias voltage.

species such as ATP and release them using electrical stimuli. It also should be noted that the Au segments without oxide layers should have helped make a good electrical contact with the electrode surfaces. We performed a control experiment using a conducting AFM to estimate the effect of Au segments on the contact resistance of NSWs (Figure S1 in the Supporting Information). The results show that the NSWs with Au segments had 600 times or lower contact resistances than those without Au segments.

Figure 3b displays the fluorescence intensity of the NSWs as a function of time. The fluorescence intensity was averaged over the NSWs as shown in Figure 3a. The fluorescence intensity increased with the application of −2 V bias voltages, but it decreased abruptly with the removal of the bias voltages. The fluorescence intensity of NSWs confirmed that the PPy-ATP segment released ATP molecules when the bias voltage was applied, while it ceased to release when the bias voltage was removed. It should be noted that, upon the application of electrical stimuli, ATP molecules could be repeatedly released from the NSWs with a short response time. It is also worth discussing the lifetime of the chemical species in NSWs. The lifetime of NSWs is expected to vary depending on the properties of stored chemical species and environmental conditions. In the case of ATP, it can be easily destroyed when moisture in the PPy segment is completely removed. We could keep the deposited NSWs under dry environments over 12 h and demonstrate the release of ATP (Figure S2a in the Supporting Information). However, we can expect that for a longer storage of ATP in the NSWs, the device should be stored in humid or wet environments. The ATP in NSWs is expected to be stored for a long time period at a low temperature just like other biological molecules. For example, we could store the NSWs with ATP in deionized water at −20 °C for 2 weeks and use them to release ATP (Figure S2b in the Supporting Information).

We performed a simulation to estimate how much ATP can be stored in each NSW and can be released from it. The detailed explanation can be found in the Supporting Information (supplementary note 1, Figure S3). In brief, the initial ATP concentration within a NSW was estimated as 0.81 M considering the dimensions of the NSWs and the concentration of the used chemical species. Then, the ATP release from the NSWs was simulated using a commercial finite element method package, COMSOL Multiphysics. We modeled our NSW system based on the thin layer diffusion model.[31,41] On the basis of the simulation result, the ATP concentration inside the PPy-ATP segment was estimated to be 0.81 M at 0 s, 0.60 M at 5 s, and 0.40 M at 10 s during the application of a negative bias voltage (Figure S3). Therefore, 12×10^{-17} mol of ATP was released from each NSW every 10 s at the initial stages. Assuming that the ATP in our present PPy-ATP patterns was used to fill our flow cell with dimensions of 1 cm × 0.8 cm × 150 μm (W × L × H), the ATP concentration in the flow cell could increase up to 119.85 μM. However, it also

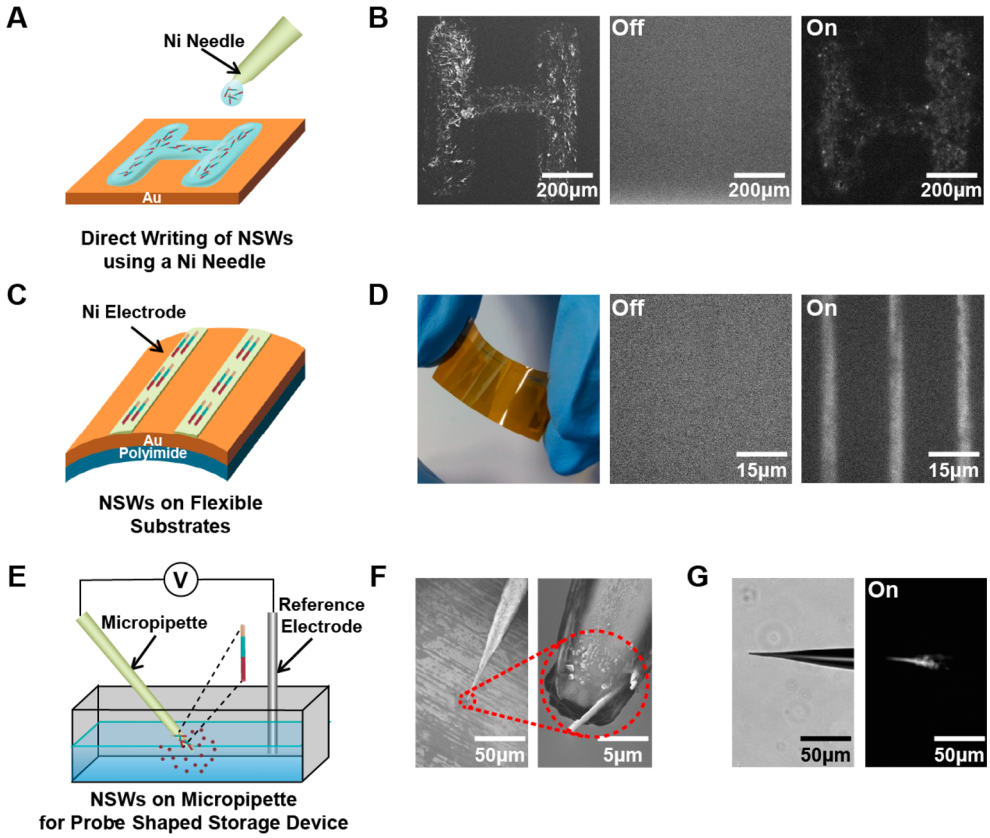

Figure 4. Printable "nano-storage" devices. (a) Schematic diagram depicting the direct writing of NSWs onto a solid substrate. "NSW ink" was written onto a Au substrate using a magnetized needle. (b) SEM image (left) of NSWs printed *via* direct writing and fluorescence image of the same sample with (right) and without (middle) the application of −2 V bias voltages. The ATP bioluminescence assay solution (luciferin/luciferase kit from Sigma Aldrich, USA) was used to detect the release of ATP. (c) Schematic diagram showing a flexible nanostorage device. Polyimide film was coated with a Au layer and Ni patterns (green). NSWs were driven and deposited on the Ni electrodes *via* external magnetic fields. (d) Photographic image (left) and fluorescence image of the flexible storage device with (right) and without (middle) a bias voltage of −2 V. (e) Schematic diagram depicting the controlled release of ATP from NSWs deposited on a micropipet. The micropipet was placed in the ATP bioluminescence kit, and then a bias voltage of −2 V was applied to release ATP from the NSWs. (f) SEM image of NSWs deposited on a micropipet. (g) Optical (left) and fluorescence (right) images of NSWs attached on a micropipet when a bias voltage of −2 V was applied.

should be noted that the maximum possible ATP concentration by our method can be increased much further simply by depositing more NSWs, implying that our method can be utilized to control the ATP concentration from zero up to a very high concentration.

The released ATP could be utilized to control the activities of protein molecules such as biomotors (Figure 3c). Here, NSWs were first deposited onto a thin Au film, and, then, the Au film was utilized as a substrate for the microtubule−kinesin motility assay.[42] When a bias voltage was applied onto the substrate, ATP was released from the NSWs. The kinesin molecules were activated, resulting in the motion of microtubules on them.[31] It is worth discussing the advantages and disadvantages of our method for the control of biomotor activities compared with previous works. Previously, a thermoelectric chip was utilized to control the localized activity of biomotors by controlling the local temperature.[43−45] This method can efficiently turn on and off all biomolecular activities related with temperature in a localized region. However, in our method, one can selectively control the biomolecular activities related with ATP or any released chemical species while leaving other biomolecular activities unaltered. Thus, our NSWs should be a new powerful tool for the selective control of specific biomolecular activities in a localized region.[17−19,43−45]

We could place individual NSWs between two electrodes for the controlled release of ATP molecules (Figure 3d). Here, an external magnetic field was applied to trap a NSW between two Ni/Au electrode patterns from its solution (details in the Materials and Methods section). Figure 3e illustrates the optical and fluorescence images of a single NSW deposited on top of two neighboring Ni/Au electrodes. The NSW was located on top of two Ni/Au neighboring electrodes as expected (left panel). The fluorescence micrograph shows that the NSW luminesced only upon application of a −2 V bias voltage (middle and right panels). In this case, since the bias voltage was applied between two nearby electrodes, an additional separate electrode was not required. Thus, we should be able to fabricate

micro- and even nanoscale storage devices based on NSWs for the controlled release of chemical species. This result also clearly shows that our device can be utilized to control the local concentration of biomolecules without any bulky equipment, which can be an advantage compared with previous methods.[7−19]

NSWs are quite versatile nanostructures that can be utilized for various chemical storage device applications for controlled release of biochemical species (Figure 4). First, we demonstrated the direct writing of NSWs on solid substrates for a printable device (Figure 4a). Here, a Ni needle was dipped into the NSW solution to form a small droplet of "NSW ink" at its end. Then, it was fixed on a probe-manipulator and used as a "pen" to directly write NSWs on the Au substrate. Figure 4b shows the SEM image (left panel) and fluorescence micrographs (middle and right panel) of NSWs prepared by this direct writing method. The SEM image shows that NSWs are deposited on the substrate in the shape of an "H". Furthermore, the "H" shape lit up when a negative bias voltage of −2 V was applied to the underlying Au substrate. This clearly shows that NSWs can be easily written onto the desired region of the substrate to build storage device structures for the controlled release of biochemical molecules.

We also demonstrated *flexible* nanostorage devices (Figure 4c). Here, NSWs were driven by magnetic fields and deposited onto Ni/Au films on a transparent and flexible polyimide film (left panel of Figure 4d). The device transmitted some light, and it can be easily bent. The middle and right panels of Figure 4d are the fluorescence images of a flexible nanostorage device without and with a −2 V bias voltage on the substrate, respectively. Note that the linear patterns containing NSWs illuminated brightly when a negative bias voltage was applied. Since the networks of NSWs are flexible and can be prepared on many different substrates including flexible substrates, it should open up various applications such as flexible storage devices for the controlled release of biochemical molecules.

The NSWs can be deposited onto *curved* surfaces such as the sharp end of a micropipet to fabricate quite versatile storage devices (Figure 4e). Here, the end of an Au-coated micropipet[46] was placed in the solution of NSWs so that NSWs adhered onto it, resulting in probe-shaped storage devices. Figure 4f shows the SEM images of NSWs at the end of the micropipet. When a negative bias voltage was applied to the micropipet, the tip region appeared bright (Figure 4g). These results indicate that the release of ATP molecules was localized at the tip of the micropipet where the NSWs were attached. Therefore, such probe-shaped storage devices can be used for the delivery of chemicals to individual cells through a direct injection. Also, these results show that we can deposit NSWs onto virtually any structure to create nanoscale devices for the controlled release of biochemical materials.

CONCLUSIONS

In conclusion, we report an NSW structure that can be deposited onto virtually any substrate to build nanostorage devices for the real-time controlled release of biochemical molecules upon the application of electrical stimuli. The NSWs were three different segments comprising PPy, ferromagnetic Ni, and conductive Au, each of which was used to store chemical species, align NSWs by magnetic fields, and make a good electrical contact to external electrodes, respectively. NSWs have been deposited onto specific locations on solid substrates *via* various methods such as direct writing or magnetic field driven assembly, and they were utilized for the controlled release of ATP. We also demonstrated the deposition of NSWs onto flexible substrates or the end of micropipets to fabricate flexible or probe-type nanostorage devices, respectively. These results clearly show that NSWs are quite versatile structures, allowing us to fabricate nanostorage devices on virtually any substrate for the controlled release of biochemical molecules. Thus, our strategy should provide great opportunities in various areas such as drug delivery systems,[8−10] biosensors,[5,6] and biochips[3] for the controlled release of chemicals to biosystems.

MATERIALS AND METHODS

Fabrication of NSWs. For the fabrication of NSWs, an anodic aluminum oxide (Anodisc, Whatman Inc., USA) membrane was used as a template. The pore size and the thickness of the AAO template were 200 nm and 60 μm, respectively. First, a 500 nm thick Ag layer was thermally evaporated onto the back side of the AAO template.[30,37] Then, the AAO template was installed on a custom-built Teflon electrochemical cell (diameter of 8 mm) and immersed in Ag plating solution (Techni Silver 1025, Technic Inc., USA). An additional Ag layer was electrochemically deposited using a potentiostat (Reference 600, Gamry Instruments Inc., USA) at a bias voltage of −0.9 V. In this process, a platinum (Pt) wire with 1 mm diameter (I-Nexus Inc., Korea) was used as a counter electrode, and an Ag/AgCl electrode (MF-2052, Bioanalytical System Inc., USA) was used as a reference electrode. The desired Au (Orotemp 24, Technic Inc., USA) and Ni (High Speed Nickel Sulfamate FFT, Technic Inc., USA) segments were sequentially deposited at a bias voltage of −0.9 V. Finally, PPy-ATP segments were deposited using pyrrole−ATP deposition solution (0.1 M pyrrole (Sigma Aldrich, USA) and 20 mM ATP (Sigma Aldrich, USA)) at a bias voltage of +0.9 V. After the completion of each deposition process, the electrochemical cell was thoroughly rinsed using deionized water. After finishing all deposition processes, the Ag backing layer was etched off using 70% nitric acid (Sigma Aldrich, USA), and then the AAO template was dissolved in 3 M NaOH solution to disperse the NSWs. The dispersed NSWs were centrifuged, and the supernatant was replaced with deionized water at least three times.

Surface Characterization of NSWs. A field emission scanning electron microscope (FE-SEM) (Hitachi 4800, Hitachi, Japan)

was used for the imaging of NSWs. The composition of NSWs was analyzed by energy dispersive X-ray spectroscopy (Hitachi 4800, Hitachi, Japan).

Magnetic Alignment of NSWs. To create Ni patterns on a cover glass, we first patterned photoresist (AZ 5214) on a cover glass *via* the conventional photolithography process, followed by the thermal evaporation of Ni (200 nm). Subsequently, the photoresist pattern was removed by dipping the substrate in acetone. Finally, the NSW solution was dropped onto the Ni patterns, and an external magnetic field (50 mT) was applied in the perpendicular direction to the plane of the substrate using a solenoid until the solution was dried.

ATP Bioluminescence Assay. For the ATP bioluminescence assay, NSW solution was dropped on a desired substrate (*i.e.*, a Ti/Au (10/30 nm)-coated glass slide), and the substrate was placed in a vacuum chamber for 1 h to dry the solution. For the fabrication of a flow cell, the NSW deposited substrate was covered with a Ti/Au (10/30 nm)-coated glass slide as a counter electrode, using 3M double-sided tape as a spacer. The ATP bioluminescence assay solution (Sigma Aldrich, USA) was prepared as recommended in the provider's manual. The assay solution was injected into the flow cell, and the negative bias voltage of −2 V was repeatedly applied for the release of ATP from the NSWs. The luminescence from the reaction was observed *via* fluorescence microscopy at an FITC channel.

Kinesin and Microtubule Preparation. Chimera kinesin (NKHK560cys) was expressed in *Escherichia coli* Rosetta 2(DE3)pLysS and purified by His-tag affinity chromatography as reported previously.[47] This chimera kinesin consisted of the head and neck domains of *Neurospara crassa* kinesin and the stalk domain of *Homo sapiens* kinesin. For the preparation of microtubules, the rhodamine-labeled tubulin (TL590M, Sigma Aldrich, USA) was mixed with the unlabeled tubulin (T240, Sigma Aldrich, USA) at the molar ratio of 5%, as previously reported.[48]

Biomotor Assay. Gliding assays were performed to observe microtubules propelled by kinesin.[49] First, NSWs were deposited on a Ti/Au (10/30 nm)-coated glass substrate, and then a flow cell was fabricated. Afterward, the flow cell was incubated with casein solution (0.5 mg mL^{-1} in BRB80 buffer) for 3 min. Then, it was incubated with kinesin solution (0.2 mg mL^{-1} kinesin, 0.5 mg mL^{-1} casein in BRB80 buffer) for 30 min. Microtubule solution containing rhodamine-labeled microtubules (0.1 μM tubulin), 20 μM Taxol, 1 mM dithiothreitol, antibleaching cocktail (3 mg mL^{-1} D-glucose, 0.1 mg mL^{-1} glucose oxidase, 0.017 mg mL^{-1} catalase), and a redox mediator (3 mM ferrocenedimethanol ($Fc(MeOH)_2$)) in BRB80 buffer was introduced to the flow cell, and the flow cell was incubated for 3 min. Since the motility of the microtubule−kinesin system is temperature sensitive,[50] the temperature was maintained at 35 °C using a microscope incubation system (INU-TIZ-F1, Tokai Hit, Japan).

Optical Imaging. Bright field and fluorescence images were observed using a microscope (TE2000U, Nikon, Japan) equipped with an EMCCD (DQC FS, Nikon, Japan) and an LED light source (CoolLED pE-1, Custom Interconnect Ltd., UK). The LED light source with an excitation wavelength of 550 nm and a TRITC filter (EX 540/25, DM 565, BA605/55, Nikon, Japan) was used for fluorescence imaging. We analyzed the fluorescence intensity from NSWs using the Metamorph analysis software (Molecular Devices, USA).

Fabrication of Single NSW-Based Devices. Ni/Au (200/30 nm) electrodes were fabricated *via* the conventional photolithography process.[27] Then, the NSW solution was dropped on the Ni/Au electrodes. Finally, a magnetic field (50 mT) was applied in the perpendicular direction to the long axis of the linear Ni/Au electrodes in order to address the individual NSW on top of two neighboring Ni/Au electrodes separated by 5 μm.

Direct Writing of NSWs. Commercially available Ni needles were magnetized inside a solenoid (50 mT) and dipped into the NSW solution (10^{10} unit mL^{-1}) so that a small droplet of the NSW solution was formed at its end. Then, the needle was installed on a probe-manipulator (MST-PM50, MS Tech., Korea) and utilized as a "pen" to directly write NSWs on a Ti/Au (10/30 nm)-coated glass substrate.

Fabrication of Flexible Devices. A commercially available Kapton polyimide film (0.2 mm, DuPont Inc., USA) was sonicated in acetone and then used to fabricate a flexible device. For the formation of a working electrode, Ti/Au (10/30 nm) layers were thermally deposited on the polyimide film. Subsequently, Ni line patterns with 100 nm thickness were fabricated on top of the Ti/Au-coated polyimide film. NSW solution (10^{10} unit mL^{-1}) was dropped on the polyimide film, while a magnetic field (50 mT) was applied along the long axis of the Ni line patterns.

Fabrication of an NSW-Coated Micropipet. Borosilicate glass capillaries with an initial inner diameter of 1.2 mm and outer diameter of 1.5 mm (World Precision Instruments Inc., USA) were used as starting materials for the fabrication of micropipets. A glass capillary was loaded on a vertical micropipet puller (PC-10, Narishige, Japan). The center of the glass capillary was preheated by applying 68 V and postheated by applying 48 V to the heater element of the puller. Then, the capillary was stretched and cut. After pulling the capillary, the surface of the micropipet was cleaned by piranha solution (H_2SO_4−H_2O_2, 4:1).[42] The entire surface of the micropipet was covered with Ti/Au (10/30 nm) layers. Finally, the end of the micropipet was dipped into the NSW solution (10^{10} unit mL^{-1}) for 5 min so that NSWs would adhere onto it.

Conflict of Interest: The authors declare no competing financial interest.

Acknowledgment. This work was supported by NRF grants (Nos. 2012-0000117, 2012-0006564). S.H. acknowledges the support from the Ministry of Science, ICT & Future Planning (Nos. 2012K001366, 2012-0009565, 2010-00293).

Supporting Information Available: This material is available free of charge via the Internet at http://pubs.acs.org.

REFERENCES AND NOTES

1. Bray, D. Protein Molecules as Computational Elements in Living Cells. *Nature* **1995**, *378*, 419–419.
2. Spudich, J. A. How Molecular Motors Work. *Nature* **1994**, *372*, 515–518.
3. Sundberg, M.; Bunk, R.; Albet-Torres, N.; Kvennefors, A.; Persson, F.; Montelius, L.; Nicholls, I. A.; Ghatnekar-Nilsson, S.; Omling, P.; Tagerud, S.; *et al*. Actin Filament Guidance on a Chip: Toward High-Throughput Assays and Lab-on-a-Chip Applications. *Langmuir* **2006**, *22*, 7286–7295.
4. Mir, M.; Homs, A.; Samitier, J. Integrated Electrochemical DNA Biosensors for Lab-on-a-Chip Devices. *Electrophoresis* **2009**, *30*, 3386–3397.
5. Jin, H. J.; Lee, S. H.; Kim, T. H.; Park, J.; Song, H. S.; Park, T. H.; Hong, S. Nanovesicle-Based Bioelectronic Nose Platform Mimicking Human Olfactory Signal Transduction. *Biosens. Bioelectron.* **2012**, *35*, 335–341.
6. Lee, B. Y.; Seo, S. M.; Lee, D. J.; Lee, M.; Lee, J.; Cheon, J. H.; Cho, E.; Lee, H.; Chung, I. Y.; Park, Y. J.; *et al*. Biosensor System-on-a-Chip Including CMOS-Based Signal Processing Circuits and 64 Carbon Nanotube-based Sensors for the Detection of a Neurotransmitter. *Lab Chip* **2010**, *10*, 894–898.
7. Tao, S. L.; Desai, T. A. Microfabricated Drug Delivery Systems: From Particles to Pores. *Adv. Drug Delivery Rev.* **2003**, *55*, 315–328.
8. George, P. M.; LaVan, D. A.; Burdick, J. A.; Chen, C. Y.; Liang, E.; Langer, R. Electrically Controlled Drug Delivery from Biotin-Doped Conductive Polypyrrole. *Adv. Mater.* **2006**, *18*, 577–581.
9. Geetha, S.; Rao, C. R. K.; Vijayan, M.; Trivedi, D. C. Biosensing and Drug Delivery by Polypyrrole. *Anal. Chim. Acta* **2006**, *568*, 119–125.
10. Ge, D. T.; Tian, X. D.; Qi, R.; Huang, S. Q.; Mu, J.; Hong, S. M.; Ye, S. F.; Zhang, X. M.; Li, D. H.; Shi, W. A Polypyrrole-Based Microchip for Controlled Drug Release. *Electrochim. Acta* **2009**, *55*, 271–275.
11. Santini, J. T.; Richards, A. C.; Scheidt, R.; Cima, M. J.; Langer, R. Microchips as Controlled Drug-Delivery Devices. *Angew. Chem., Int. Ed.* **2000**, *39*, 2397–2407.
12. Razzacki, S. Z.; Thwar, P. K.; Yang, M.; Ugaz, V. M.; Burns, M. A. Integrated Microsystems for Controlled Drug Delivery. *Adv. Drug Delivery Rev.* **2004**, *56*, 185–198.

13. Saltzman, W. M.; Olbricht, W. L. Building Drug Delivery into Tissue Engineering. *Nat. Rev. Drug Discovery* **2002**, *1*, 177–186.
14. Goldman, E. W.; Hibberd, M. G.; McCray, J. A.; Trentham, D. R. Releaxation of Muscle Fibers by Photolysis of Caged ATP. *Nature* **1982**, *300*, 701–705.
15. Goldman, E. W.; Hibberd, M. G.; Trentham, D. R. Relaxation of Rabbit Psoas Muscle Fibres from Rigor by Photochemical Generation of Adenosine-5′-Triphosphate. *J. Physiol.* **1984**, *354*, 577–604.
16. Dantzig, J. A.; Goldman, Y. E.; Millar, N. C.; Lacktis, J.; Homsher, E. Reversal of the Cross-Bridge Force-Generating Transition by Photogeneration of Phosphate in Rabbit Psoas Muscle Fibers. *J. Physiol.* **1992**, *451*, 247–278.
17. Goldman, Y. E; Hibberd, M. G.; Trentham, D. R. Relaxation of Rabbit Psoas Muscle Fibres from Rigor by Photochemical Generation of Adenosine-5′-Triphosphate. *J. Physiol.* **1984**, *354*, 577–604.
18. Hess, H.; Clemmens, J.; Qin, D.; Howard, J.; Vogel, V. Light-Controlled Molecular Shuttles Made from Motor Proteins Carrying Cargo on Engineered Surfaces. *Nano Lett.* **2001**, *1*, 235–239.
19. Grove, T. J.; Puckett, K. A.; Brunet, N. M.; Mihajlovic, M.; McFadden, L. A.; Xiong, P.; von Molnar, S.; Moerland, T. S.; Chase, P. B. Packaging Actomyosin-Based Biomolecular Motor-Driven Devices for Nanoactuator Applications. *IEEE Trans. Adv. Packag.* **2005**, *28*, 556–563.
20. Paciotti, G. F.; Kingston, D. G. I.; Tamarkin, L. Colloidal Gold Nanoparticles: A Novel Nanoparticle Platform for Developing Multifunctional Tumor-Targeted Drug Delivery Vectors. *Drug Dev. Res.* **2006**, *67*, 47–54.
21. Gelperina, S.; Kisich, K.; Iseman, M. D.; Heifets, L. The Potential Advantages of Nanoparticle Drug Delivery Systems in Chemotherapy of Tuberculosis. *Am. J. Resp. Crit. Care* **2005**, *172*, 1487–1490.
22. Paciotti, G. F.; Myer, L.; Weinreich, D.; Goia, D.; Pavel, N.; McLaughlin, R. E.; Tamarkin, L. Colloidal Gold: A Novel Nanoparticle Vector for Tumor Directed Drug Delivery. *Drug Delivery* **2004**, *11*, 169–183.
23. Sharma, H. S.; Ali, S. F.; Dong, W.; Tian, Z. R.; Patnaik, R.; Patnaik, S.; Sharma, A.; Boman, A.; Lek, P.; Seifert, E.; Lundstedt, T. Drug Delivery to the Spinal Cord Tagged with Nanowire Enhances Neuroprotective Efficacy and Functional Recovery Following Trauma to the Rat Spinal Cord. *Ann. N.Y. Acad. Sci.* **2007**, *1122*, 197–218.
24. Fischer, K. E.; Aleman, B. J.; Tao, S. L.; Daniels, R. H.; Li, E. M.; Bunger, M. D.; Nagaraj, G.; Singh, P.; Zettl, A.; Desai, T. A. Biomimetic Nanowire Coatings for Next Generation Adhesive Drug Delivery Systems. *Nano Lett.* **2009**, *9*, 716–720.
25. Fan, Z. Y.; Ho, J. C.; Takahashi, T.; Yerushalmi, R.; Takei, K.; Ford, A. C.; Chueh, Y. L.; Javey, A. Toward the Development of Printable Nanowire Electronics and Sensors. *Adv. Mater.* **2009**, *21*, 3730–3743.
26. Fan, Z. Y.; Ho, J. C.; Jacobson, Z. A.; Yerushalmi, R.; Alley, R. L.; Razavi, H.; Javey, A. Wafer-Scale Assembly of Highly Ordered Semiconductor Nanowire Arrays by Contact Printing. *Nano Lett.* **2008**, *8*, 20–25.
27. Bangar, M. A.; Hangarter, C. M.; Yoo, B.; Rheem, Y.; Chen, W.; Mulchandani, A.; Myung, N. V. Magnetically Assembled Multisegmented Nanowires and Their Applications. *Electroanalysis* **2009**, *21*, 61–67.
28. Wanekaya, A. K.; Chen, W.; Myung, N. V.; Mulchandani, A. Nanowire-Based Electrochemical Biosensors. *Electroanalysis* **2006**, *18*, 533–550.
29. Kovtyukhova, N. I.; Mallouk, T. E. Nanowires as Building Blocks for Self-Assembling Logic and Memory Circuits. *Chem.—Eur. J.* **2002**, *8*, 4355–4363.
30. Qin, L. D.; Park, S.; Huang, L.; Mirkin, C. A. On-Wire Lithography. *Science* **2005**, *309*, 113–115.
31. Byun, K. E.; Choi, D. S.; Kim, E.; Seo, D. H.; Yang, H.; Seo, S.; Hong, S. Graphene-Polymer Hybrid Nanostructure-Based Bioenergy Storage Device for Real-Time Control of Biological Motor Activity. *ACS Nano* **2011**, *5*, 8656–8664.
32. Pernaut, J. M.; Reynolds, J. R. Use of Conducting Electroactive Polymers for Drug Delivery and Sensing of Bioactive Molecules. A Redox Chemistry Approach. *J. Phys. Chem. B* **2000**, *104*, 4080–4090.
33. Xiao, Y. H.; Che, J. F.; Li, C. M.; Sun, C. Q.; Chua, Y. T.; Lee, V. S.; Luong, J. H. T. Preparation of Nano-Tentacle Polypyrrole with Pseudo-Molecular Template for ATP Incorporation. *J. Biomed. Mater. Res. A* **2007**, *80A*, 925–931.
34. Tanase, M.; Silevitch, D. M.; Hultgren, A.; Bauer, L. A.; Searson, P. C.; Meyer, G. J.; Reich, D. H. Magnetic Trapping and Self-Assembly of Multicomponent Nanowires. *J. Appl. Phys.* **2002**, *91*, 8549–8551.
35. Ye, H.; Gu, Z.; Y, T.; Gracias, D. H. Integrating Nanowires with Substrates Using Directed Assembly and Nanoscale Soldering. *IEEE Trans. Nanotechnol.* **2006**, *5*, 62–66.
36. Critchley, K.; Khanal, B. P.; Górzny, M. Ł.; Vigderman, L.; Evans, S. D.; Zubarev, E. R.; Kotov, N. A. Near-Bulk Conductivity of Gold Nanowires as Nanoscale Interconnects and the Role of Atomically Smooth Interface. *Adv. Mater.* **2010**, *22*, 2338–2342.
37. Lee, B. Y.; Heo, K.; Schmucker, A. L.; Jin, H. J.; Lim, J. K.; Kim, T.; Lee, H.; Jeon, K. S.; Suh, Y. D.; Mirkin, C. A.; *et al.* Nanotube-Bridged Wires with Sub-10 nm Gaps. *Nano Lett.* **2012**, *12*, 1879–1884.
38. Williams, K. R.; Gupta, K.; Wasilik, M. Etch Rates for Micromachining Processing - Part II. *J. Microelectromech. Syst.* **2003**, *12*, 761–778.
39. Lopez Cascales, J. J.; Otero, T. F. Molecular Dynamic Simulation of the Hydration and Diffusion of Chloride Ions from Bulk Water to Polypyrrole Matrix. *J. Chem. Phys.* **2004**, *120*, 1951–1957.
40. Lopez Cascales, J. J.; Fernandez, A. J.; Otero, T. F. Characterization of the Reduced and Oxidized Polypyrrole/Water Interface: A Molecular Dynamics Simulation Study. *J. Phys. Chem. B* **2003**, *107*, 9339–9343.
41. Siepmann, J.; Ainaoui, A.; Vergnaud, J. M.; Bodmeier, R. Calculation of the Dimensions of Drug-Polymer Devices Based on Diffusion Parameters. *J. Pharm. Sci.* **1998**, *87*, 827–832.
42. van den Heuvel, M. G. L.; Butcher, C. T.; Lemay, S. G.; Diez, S.; Dekker, C. Electrical Docking of Microtubules for Kinesin-Driven Motility in Nanostructures. *Nano Lett.* **2005**, *5*, 235–241.
43. Nomura, A.; Uyeda, T. Q. P.; Yumoto, N.; Tatsu, Y. Photo-Control of Kinesin-Microtubule Motility Using Caged Peptides Derived from the Kinesin C-Terminus Domain. *Chem. Commun.* **2006**, 3588–3590.
44. Mihajlovic, G.; Brunet, N. M.; Trbovic, J.; Xiong, P.; Von Molnar, S.; Chase, P. B. All-Electrical Switching and Control Mechanism for Actomyosin-Powered Nanoactuators. *Appl. Phys. Lett.* **2004**, *85*, 1060–1062.
45. Ionov, L.; Stamm, M.; Diex, S. Reversible Switching of Microtubule Motility Using Thermosensitive Polymer Surfaces. *Nano Lett.* **2006**, *6*, 1982–1987.
46. Son, D.; Park, S. Y.; Kim, B.; Koh, J. T.; Kim, T. H.; An, S.; Jang, D.; Kim, G. T.; Jhe, W.; Hong, S. Nanoneedle Transistor-Based Sensors for the Selective Detection of Intracellular Calcium Ions. *ACS Nano* **2011**, *5*, 3888–3895.
47. Cheng, L. J.; Kao, M. T.; Meyhöfer, E.; Guo, L. J. Highly Efficient Guiding of Micortubules in Imprinted Nanotracks. *Small* **2005**, *1*, 409–414.
48. Choi, D. S.; Byun, K. Y.; Hong, S. Dual Transport Systems Based on Hybrid Nanostructures of Microtubules and Actin Filaments. *Small* **2011**, *7*), 1755–1760.
49. Howard, J.; Hunt, A. J.; Baek, S. Kinesin Swivels to Permit Microtubule Movement in any Direction. *Methods Cell Biol.* **1993**, *39*, 137–147.
50. Böhm, K. J.; Stracke, R.; Baum, M.; Zieren, M.; Unger, E. Effect of Temperature on Kinesin-Driven Microtubule Gliding and Kinesin ATPase Activity. *FEBS Lett.* **2000**, *46*, 59–62.